A Bis(diimidazole)copper Complex Possessing a Reversible Cu^{II}/Cu^{I} Couple with a High Redox Potential

Jonathan McMaster, Roy L. Beddoes, David Collison, David R. Eardley, Madeleine Helliwell and C. David Garner*

Abstract: The new diimidazole ligand, bis(1-methyl-4,5-diphenylimidazol-2-yl)ketone (BIMDPK), has been synthesised, characterised and shown to form four-coordinate bis(diimidazole) Cu^{II} and Cu^{I} complexes in the salts $[Cu(bimdpk)_2][BF_4]_2$ and $[Cu(bimdpk)_2][PF_6]$, the structures of which have been determined by X-ray crystallography. The cations of these salts have a very similar geometry with $Cu^{II}-N_{av} = 1.949$ and $Cu^{I}-N_{av} = 1.999$ Å; the N-Cu-N interbond angles are constrained by 1) the bite angle of the BIMDPK ligand to $94 \pm 2°$ and 2) the interligand steric interactions, which lead to the dihedral angle of the intraligand CuN_2 planes of 68.2° for Cu^{II} and 74.9° for Cu^{I}—that is, a CuN_4 geometry intermediate between tetrahedral and square planar. The X-band EPR spectrum for the powdered Cu^{II} compound is typical of an approximately D_2 CuN_4 centre possessing a d_{xy} ground state ($g_x = 2.080$, $g_y = 2.075$, $g_z = 2.291$; $A_z = 112.3 \times 10^{-4}\ cm^{-1}$). The UV/vis spectra are dominated by charge-transfer bands, and both the Cu^{II} and Cu^{I} systems are intensely coloured. The EPR and electronic spectra indicate that these cations have a very similar structure in the solid state and in solution; the potential of the $[Cu(bimdpk)_2]^{2+}/[Cu(bimdpk)_2]^{+}$ couple is 0.59 V vs. SCE in MeCN and 0.80 V vs. SCE in CH_2Cl_2, and the electron self-exchange constant in MeCN is $1.9 \times 10^4\ M^{-1}\ s^{-1}$. Comparisons are made between the properties of the $[Cu(bimdpk)_2]^{2+/+}$ centres and related Cu centres in chemical and biological systems; the results of this study reinforce the view that a $[Cu(His)_4]$ centre should not be precluded from consideration in biological electron transport.

Keywords
copper complexes · imidazole ligands · redox systems · structure elucidation · enzyme models

Introduction

Imidazole is a ubiquitous ligand for 3d metal ions bound to proteins.[1] Copper–imidazole ligation has been demonstrated in many metalloproteins and enzymes including plastocyanin,[2] azurin,[3] superoxide dismutase,[4] galactose oxidase,[5] haemocyanin,[6] copper nitrite reductase[7] and ascorbate oxidase.[8] In the blue, Type I copper proteins plastocyanin and azurin, the active-site structure comprises the trigonal array $[CuN_2S]$ of two histidine ligands and one cysteine ligand about the copper, together with a weak axial methionine interaction. This coordination geometry is largely retained in the oxidised and reduced forms of these proteins.[9, 10] Furthermore, in both forms the active-site geometry is considerably removed from the normally preferred geometries of Cu^{II} (tetragonal/square planar) and Cu^{I} (tetrahedral).[10] The oxidised form of Cu/Zn bovine superoxide dismutase (Cu^{II}ZnSOD) involves Cu^{II} coordinated by three imidazoles (from His 44, 46 and 118) and an imidazolate (from His 61), which bridges to the Zn^{II}; this CuN_4 centre has a geometry intermediate between square planar and tetrahedral.[4] In addition, a fifth axial coordination position is occupied by H_2O.[11, 12] Protein crystallography[13] has shown that this geometry is retained upon reduction to Cu^{I} (Cu^{I}ZnSOD), although solution NMR[14] and EXAFS[15] studies indicate that the His 61 is cleaved from the copper by protonation to produce a three-coordinate Cu^{I} site.

Many low molecular weight copper tetrakis(imidazole) complexes have been characterised and used to examine the chemistry that controls the peculiar geometry, spectroscopy and reactivity of these important copper proteins.[16–19] Although there is a precedent for the preparation of copper complexes with equivalent ligation in the oxidised and reduced forms,[19–21] only one diimidazole ligand, 2,2′-bis[2-imidazolyl]biphenyl [$(imid)_2bp$], has been shown previously to yield tetrakis(imidazole), four-coordinate Cu^{II} and Cu^{I} complexes with similar structures, which are intermediate between square-planar and tetrahedral geometries.[19] We have initiated a programme concerned with the synthesis of di- and triimidazole ligands, designed to control the coordination chemistry at metal centres. Herein, we report a three-step synthesis of the diimidazole ligand bis(1-methyl-4,5-diphenylimidazol-2-yl) ketone (BIMDPK) (Fig. 1) and its coordination to both Cu^{II} and Cu^{I}.

Experimental Procedure

Materials: All reagents and solvents were obtained from normal commercial sources and used without further purification unless otherwise stated. MeCN and CH_2Cl_2 were distilled from CaH_2, MeOH was distilled from magnesium and THF was distilled from sodium. $[Cu(MeCN)_4][PF_6]$ was prepared immediately prior to use by a literature method [22] and stored under dinitrogen. $[NnBu_4][BF_4]$ was prepared from $Na[BF_4]$ and $[NnBu_4][HSO_3]$ and recrystallised from toluene [23].

Dr. D. R. Eardley, Dr. M. Helliwell
Chemistry Department, Manchester University, Manchester M13 9PL (UK)
Fax: Int. code +(161)275-4616

  0947-6539/96/0206-0685 $ 15.00+.25/0

Analyses and Spectroscopic Methods: Chemical analyses were performed by the University of Manchester, Microanalytical Laboratory. IR spectra were recorded on a Perkin Elmer 1710 FT spectrometer. Electron impact mass spectra (EIMS) were obtained by use of a VG2000 Trio spectrometer. UV/vis spectra were recorded on a Shimadzu UV-260 spectrophotometer, and X-band EPR spectra on a Varian 112 instrument fitted with a finger dewar for frozen solution measurements. The X-band EPR spectra were simulated using an "in-house" simulation program [24]. ^{1}H NMR spectra were measured on a Varian Gemini 200 spectrometer, and ^{13}C NMR spectra were obtained on a Bruker AC300 spectrometer.

Electrochemical Measurements: Electrochemical measurements were made with a PAR model 175 waveform generator, a model 173 potentiostat and a PAR electrochemistry cell with a three-electrode configuration consisting of a glassy carbon working electrode, a standard saturated calomel reference electrode (SCE) and a platinum wire secondary electrode. All solutions were deoxygenated by bubbling dinitrogen through them for several minutes prior to use. All voltammograms were recorded with the solutions under a dinitrogen atmosphere. Controlled potential electrolysis (CPE) was carried out in a two-compartment cell separated by Vycor porous glass. The working and secondary electrodes were of platinum mesh. All electrochemical potentials were measured relative to SCE and were corrected for liquid-junction potentials via the use of the Fc^+/Fc (Fc = ferrocene) couple as an internal redox standard on the basis that $E(Fc^+/Fc)$ is ca. +400 mV in all solvents vs. the normal hydrogen electrode (NHE(H_2O)) [25], and the potential difference of NHE(H_2O) vs. SCE is −0.24 V.

4,5-Diphenylimidazole (Fig. 1): Benzoin (80 g, 0.37 mol) and formamide (160 mL, 4.03 mol) were placed in a 1 L round-bottomed flask and heated at reflux for 1.5 h. The reaction mixture was allowed to cool down to room temperature, and crude

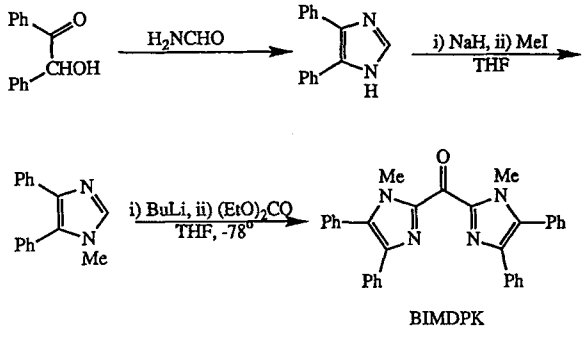

Fig. 1. Synthesis of bis(1-methyl-4,5-diphenylimidazol-2-yl) ketone (BIMDPK).

product crystallised. This was collected by filtration, washed with Et_2O and recrystallised from hot EtOH. Yield: 51.22 g (63%); m.p. 233–235 °C (ref. [26]: 231 °C); ^{1}H NMR (200 MHz, [D_6]acetone, 25 °C): δ = 7.10–7.65 (m, 12H); MS (EI) m/z (%): 220 (50) [M^+]; IR (KBr disc): $\tilde{\nu}$ = 3058 (s), 1605 (s), 1498 (s), 1462 (s), 1442 (s) cm^{-1}; $C_{15}H_{12}N_2$ (220.3): calcd C 81.8, H 5.9, N 12.7; found C 81.8, H 5.5, N 13.1.

***N*-Methyl-4,5-diphenylimidazole**: 4,5-Diphenylimidazole (16.96 g, 0.08 mol) was suspended in dry, degassed THF (100 mL) under an Ar atmosphere. Sodium hydride (3.60 g, 0.15 mol) was added cautiously in portions (0.5 g) over a period of 10 min. The reaction mixture was left to stir for a further 10 min before MeI (9 mL, 0.14 mol) was added. After having been stirred at room temperature for 1 h, the reaction was quenched by the cautious addition of an EtOH/*i*PrOH mixture (2:1 v/v, 20 mL) followed by H_2O (500 mL). The precipitated product was collected by filtration, dissolved in CH_2Cl_2 and dried over anhydrous $MgSO_4$. The solvent was removed under reduced pressure, and the product recrystallised from toluene. Yield: 13.38 g (71%); m.p. 163–165 °C; ^{1}H NMR (200 MHz, $CDCl_3$, 25 °C): δ = 3.45 (s, 3H), 7.65–7.05 (m, 11H); MS (EI) m/z (%): 234 (100) [M^+]; IR (KBr disc): $\tilde{\nu}$ = 3452 (s), 1601 (s), 1483 (s), 1444 (s) cm^{-1}; $C_{16}H_{14}N_2$ (234.3): calcd C 82.0, H 6.0, N 12.0; found C 81.7, H 6.1, N 12.4.

Bis(1-methyl-4,5-diphenylimidazol-2-yl) Ketone (BIMDPK): *N*-Methyl-4,5-diphenylimidazole (5.08 g, 22 mmol) was dissolved in dry, degassed THF (100 mL), and the solution cooled to −78 °C in an acetone/dry-ice bath under an Ar atmosphere. *n*BuLi (1.6 M in hexane, 14 mL, 22 mmol) was added dropwise over a period of 10 min, and the reaction mixture left to stir at −78 °C for 1 h. Dry, degassed diethyl carbonate (1.3 mL, 10.7 mmol) was added, and the reaction mixture left to attain room temperature over a period of 1 h. The solvent was removed by rotary evaporation, and H_2O (100 mL) was added to the residue. The bright yellow product was collected by filtration, washed with EtOH (3 × 20 mL) and recrystallised from a CH_2Cl_2/Et_2O (1:1 v/v) mixture. Attempts to complex BIMDPK (0.19 g, 0.38 mmol) with $NiCl_2 \cdot 6H_2O$ (0.20 g, 0.84 mmol) in EtOH (20 mL) resulted in the isolation of yellow crystals of BIMDPK suitable for X-ray crystallography. Yield: 4.13 g (76%); m.p. 269–272 °C; ^{1}H NMR (200 MHz, $CDCl_3$, 25 °C): δ = 3.85 (s, 6H), 7.15–7.65 (m, 20H); ^{13}C NMR (75 MHz, $CDCl_3$, 25 °C): δ = 33.8, 127.0, 127.7, 128.1, 129.2, 129.3, 129.7, 130.8, 133.9, 135.1, 140.2, 143.6, 175.0; MS (EI) m/z (%): 494 (67) [M^+]; IR (KBr disc): $\tilde{\nu}$ = 1623 (C=O, s), 1506 (s), 1493 (s), 1453 (s) cm^{-1}; $C_{33}H_{26}N_4O$ (494.6): calcd C 80.1, H 5.3, N 11.3; found C 79.8, H 5.6, N 11.4.

$Cu(BF_4)_2 \cdot 4.5H_2O$: HBF_4 (48% in H_2O) was added to excess $CuCO_3$ and allowed to react in a large crystallising dish overnight. The unreacted $CuCO_3$ was removed by filtration, and the filtrate evaporated to dryness on a rotary evaporator. The solid product was dried by heating on a vacuum line. $CuB_2F_8H_9O_{4.5}$ (318.2): calcd Cu 19.9, B 6.8, H 2.9; found Cu 20.6, B 7.2, H 3.1.

Bis[bis(1-methyl-4,5-diphenylimidazol-2-yl) ketone]copper(II) Bis(tetrafluoroborate) ($[Cu(bimdpk)_2][BF_4]_2$): A solution of $Cu(BF_4)_2 \cdot 4.5H_2O$ (0.069 g, 0.22 mmol) in EtOH was added dropwise to a solution of BIMDPK (0.200 g, 0.40 mmol) in EtOH/CH_2Cl_2 (1:1 v/v, 10 mL). After the mixture had been stirred for 30 min at room temperature, a green insoluble precipitate formed. This was collected by filtration, washed with EtOH and then Et_2O. Slow liquid diffusion of Et_2O into a solution of the product in CH_2Cl_2 at room temperature gave emerald green, block-shaped crystals suitable for X-ray crystallography. $C_{66}H_{52}N_8O_2B_2F_8Cu$ (1226.4): calcd C 64.6, H 4.3, N 9.2, B 1.8, Cu 5.2; found C 64.4, H 3.9, N 9.0, B 2.0, Cu 4.8.

Bis[bis(1-methyl-4,5-diphenylimidazol-2-yl) ketone]copper(I) Hexafluorophosphate ($[Cu(bimdpk)_2][PF_6]$): A solution of BIMDPK (0.120 g, 0.24 mmol) in dry MeOH was treated with $[Cu(MeCN)_4][PF_6]$ (0.138 g, 0.37 mmol) and stirred for 30 min. Slow evaporation of the deep blue solution at 4 °C gave dark blue, block-shaped crystals suitable for X-ray crystallography. $C_{66}H_{52}N_8O_2PF_6Cu$(1197.7): calcd C 66.2, H 4.3, N 9.4, P 2.6, Cu 5.3; found C 66.1, H 4.2, N 9.6, P 2.4, Cu 5.0.
For the complexation reactions the initial yields prior to (re)crystallisation were 30–50%.

X-ray Diffraction Studies [27]: Data collection for BIMDPK, $[Cu(bimdpk)_2][BF_4]_2$ and $[Cu(bimdpk)_2][PF_6]$ was performed on a Rigaku AFC5R four-circle diffractometer with graphite-monochromated $Cu_{K\alpha}$ radiation and a 12 kW rotating anode generator using the $\omega/2\theta$ scanning technique. Selected crystallographic data for BIMDPK, $[Cu(bimdpk)_2][BF_4]_2$ and $[Cu(bimdpk)_2][PF_6]$ are summarised in Table 1. For each crystal the intensities of three representative reflections were measured every 150 reflections and a linear correction applied to account for the intensity decay. The data were corrected for absorption, Lorentz and polarisation effects by using the program DIFABS [28a]. The non-hydrogen atoms were refined anisotropically. Hydrogen atoms were included in the structure-factor calculation in idealised positions (C–H = 0.95 Å), and were assigned isotropic thermal parameters that were 20% greater than the equivalent B value of the atom to which they were bonded.

Table 1. Crystallographic data for the compounds BIMDPK, $[Cu(bimdpk)_2][BF_4]_2$ and $[Cu(bimdpk)_2][PF_6]$ [a].

	BIMDPK	$[Cu(bimdpk)_2][BF_4]_2 \cdot CH_2Cl_2$	$[Cu(bimdpk)_2][PF_6]$
formula	$C_{33}H_{26}N_4O$	$C_{67}H_{54}N_8CuO_2B_2F_8Cl_2$	$C_{66}H_{52}N_8CuO_2PF_6$
fw	494.60	1311.28	1197.70
cryst. size/mm^3	0.20 × 0.20 × 0.20	0.22 × 0.22 × 0.22	0.30 × 0.20 × 0.20
space group	$P2_1/n$ (no. 14)	$C2$ (no. 5)	$C2/c$ (no. 15)
cryst. syst.	monoclinic	monoclinic	monoclinic
a/Å	15.264(3)	18.521(3)	30.451(7)
b/Å	10.501(4)	20.08(1)	24.76(1)
c/Å	16.502(4)	9.584(4)	21.68(1)
β/°	96.14(2)	117.30(1)	129.25(1)
V/Å^3	2630(1)	3167(4)	12656.76(18.44)
Z	4	2	8
T/K	296 ± 1	295 ± 1	295 ± 1
$\lambda(Cu_{K\alpha})$/Å	1.54178	1.54178	1.54178
ρ_{calcd}/g cm^{-3}	1.441	1.375	1.257
μ/cm^{-1}	15.6	18.9	12.6
trans. coeff.	0.85–1.00	0.74–1.19	0.82–1.20
$2\theta_{max}$/°	123.3	120.1	120.2
measured refl.	3958	2499	9942
unique refl.	3785	2415	9680
obs. refl., $I > 3.00\sigma(I)$	2661	2042	4658
no. of parameters	421	411	760
resid. e. density/e Å^{-3}	−0.24/0.26	−0.29/0.46	−0.39/0.49
$R(F_o)$	0.074	0.063	0.070
$R_w(F_o)$	0.097	0.075	0.076

[a] $R = \sum||F_o| - |F_c||/\sum|F_o|$; $R_w = [(\sum w(|F_o| - |F_c|)^2/\sum wF_o^2)]^{1/2}$, $w = 4F_o^2/\sigma^2(F_o^2)$.

0947-6539/96/0206-0686 $ 15.00+.25/0 Chem. Eur. J. 1996, 2, No. 6

A yellow crystal of BIMDPK ($C_{33}H_{26}N_4O$) was mounted on a glass fibre. The structure was solved by direct methods with the program SHELXS-86 [28b]. The space group was determined to be $P2_1/n$ (no. 14). The final cycle of full-matrix least-squares refinement converged with $R = 0.074$ and $R_w = 0.097$. The maximum and minimum peaks on the final difference Fourier map corresponded to 0.26 and $-0.24\ e\,Å^{-3}$.

A green crystal of $[Cu(bimdpk)_2][BF_4]_2 \cdot CH_2Cl_2$ ($C_{67}H_{54}N_8CuO_2B_2F_8Cl_2$) was mounted on a glass fibre. The structure was solved by direct methods with the program SHELXS-86.[28b] The space group was determined to be $C2$ (no. 5). The asymmetric unit consisted of half the molecule with Cu1, O1, O2, C1 and C18 lying on a twofold axis. In addition to the copper-containing cation, the asymmetric unit contained two half $[BF_4]^-$ anions and half a molecule of CH_2Cl_2. For one $[BF_4]^-$ counterion there is some disorder: three positions were found for the F atoms, one of which lay on a twofold symmetry axis, so that expansion through the twofold gave five positions for F. The CH_2Cl_2 molecule is disordered over two sites related by rotation. The non-hydrogen atoms were refined anisotropically, except for B1, B2 and C36 which were refined isotropically. The hydrogen atoms of the CH_2Cl_2 molecule were not included in the structure-factor calculation. Tests were made to see if the absolute configuration could be determined by carrying out the refinement on both enantiomers, but only small differences were observed for the R factors. Refinement was completed on the enantiomer with the lower R factor. The final cycle of full-matrix least-squares refinement converged with $R = 0.063$ and $R_w = 0.075$. The maximum and minimum peaks on the final difference Fourier map corresponded to 0.46 and $-0.29\ e\,Å^{-3}$.

A blue crystal of $[Cu(bimdpk)_2][PF_6]$ ($C_{66}H_{52}N_8CuO_2PF_6$) was mounted on a glass fibre. The structure was solved by direct methods with the program SHELXS-86 [28b]. The space group was determined to be $C2/c$ (no. 15). $[PF_6]^-$ occupies two sites; for the first P1 is located on a centre of symmetry; for the second, P2 is located on a twofold axis as are two of the fluorine atoms, F6 and F7. The final cycle of full-matrix least-squares refinement converged with $R = 0.070$ and $R_w = 0.076$. The maximum and minimum peaks on the final difference Fourier map corresponded to 0.49 and $-0.39\ e\,Å^{-3}$.

Results

Ligand Synthesis and Structure: BIMDPK was prepared from 1-methyl-4,5-diphenylimidazolyllithium and diethyl carbonate in 76% yield (Fig. 1), by using an adapted procedure for the

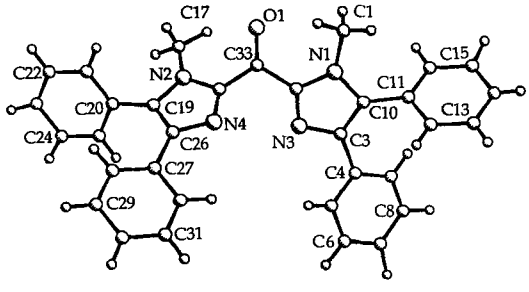

Fig. 2. A PLUTO view of the ligand BIMDPK.

preparation of bis(*N*-methylimidazol-2-yl)methanone.[29] *N*-methyl-4,5-diphenylimidazole was prepared from the previously reported 4,5-diphenylimidazole.[26] The molecular structure of the ligand is shown in Figure 2 and selected bond lengths, bond angles and dihedral angles are presented in Table 2. The structure shows the ligand ideally poised to chelate to a metal through the N3 and N4 atoms of the imidazole rings (contact distance: 3.027 Å). A dihedral angle of 54.9° between the planes of these rings indicates that the imidazole groups are not coplanar in the solid-state structure. In addition the average dihedral angles between the imidazole ring and the 5-phenyl ring (57.0°) and between the imidazole ring and the 4-phenyl ring (29.4°) demonstrate that none of the aromatic rings in BIMDPK are coplanar.

Preparation and Crystal Structures of $[Cu(bimdpk)_2][BF_4]_2$ and $[Cu(bimdpk)_2][PF_6]$: The reaction of BIMDPK with $Cu(BF_4)_2 \cdot 4.5H_2O$ or $[Cu(MeCN)_4][PF_6]$ yields $[Cu(bimdpk)_2][BF_4]_2$ or $[Cu(bimdpk)_2][PF_6]$, respectively—Cu^{II} and Cu^{I} complexes with equivalent ligation. The geometry about the metal centres is illustrated in Figures 3 and 4 and selected bond lengths and bond angles are given in Table 3. In both $[Cu(bimdpk)_2][BF_4]_2$ and $[Cu(bimdpk)_2][PF_6]$ the anions are well removed

Table 2. Bond lengths (Å), bond angles (°) and dihedral angles (°) for BIMDPK (e.s.d.'s in parentheses).

Bond lengths					
C33–O1	1.224(5)	N2–C18	1.369(5)	N4–C18	1.317(5)
C1–N1	1.454(5)	N2–C19	1.383(5)	N4–C26	1.361(5)
N1–C2	1.377(5)	N3–C2	1.325(5)	C2–C33	1.476(6)
N1–C10	1.382(5)	N3–C3	1.366(5)	C18–C33	1.458(6)
N2–C17	1.455(7)	C3–C10	1.376(5)	C19–C26	1.384(6)
Bond angles					
C1-N1-C2	127.5(4)	N1-C2-N3	112.1(4)	N2-C18-C33	122.7(4)
C1-N1-C10	126.3(4)	N1-C2-C33	123.4(4)	N4-C18-C33	126.0(4)
C2-N1-C10	106.0(3)	N3-C2-C33	124.1(4)	N4-C26-C19	109.4(4)
C17-N2-C18	126.5(4)	N3-C3-C4	119.9(4)	O1-C33-C2	121.4(4)
C18-N2-C19	106.7(4)	N3-C3-C10	110.9(4)	O1-C33-C18	123.1(4)
C2-N3-C3	105.1(3)	N1-C10-C3	105.8(4)	C2-C33-C18	115.5(4)
C18-N4-C26	107.0(4)	N2-C18-N4	111.0(4)		
Average dihedral angles [a]					
meim/4-Ph	29.4	meim/5-Ph	57.0	meim/meim	54.9

[a] Meim: *N*-methylimidazole ring plane; Ph: phenyl ring plane.

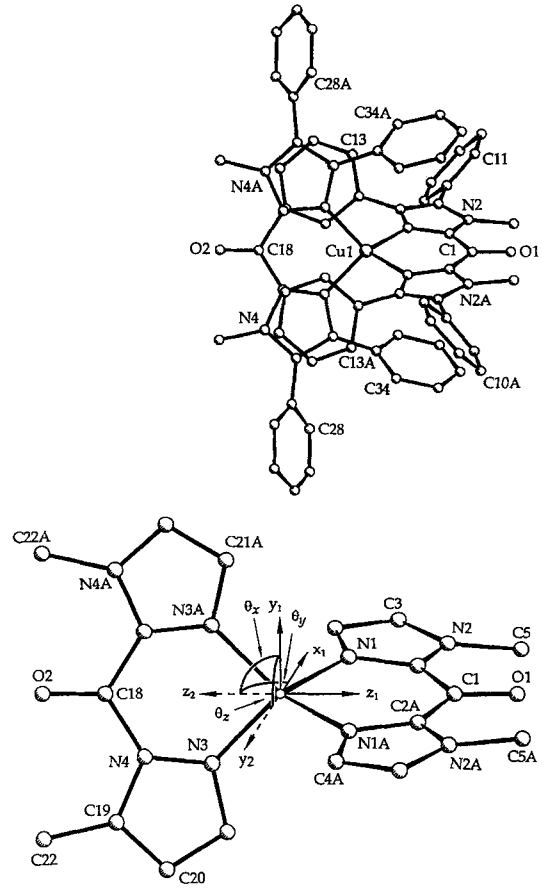

Fig. 3. PLUTO views of the $[Cu(bimdpk)_2]^{2+}$ cation in $[Cu(bimdpk)_2][BF_4]_2$, including phenyl groups (top) and with the phenyl groups removed and showing the axis system to which θ_x, θ_y and θ_z are related (bottom). The orthonormal unit vectors x_1, y_1 and z_1 are chosen so that N1, Cu and N1A lie in the x_1z_1 plane with z_1 along the bisector of angle N1-Cu-N1A. The unit vector z_2 lies along the bisector of N3-Cu-N3A. The unit vector y_2 is defined as being perpendicular to the N3/Cu/N3A plane. θ_x is the angle between z_2 and y_1, θ_y between z_2 and x_1 and θ_z between y_2 and y_1. The latter defines the dihedral angle between intraligand CuN_2 planes.

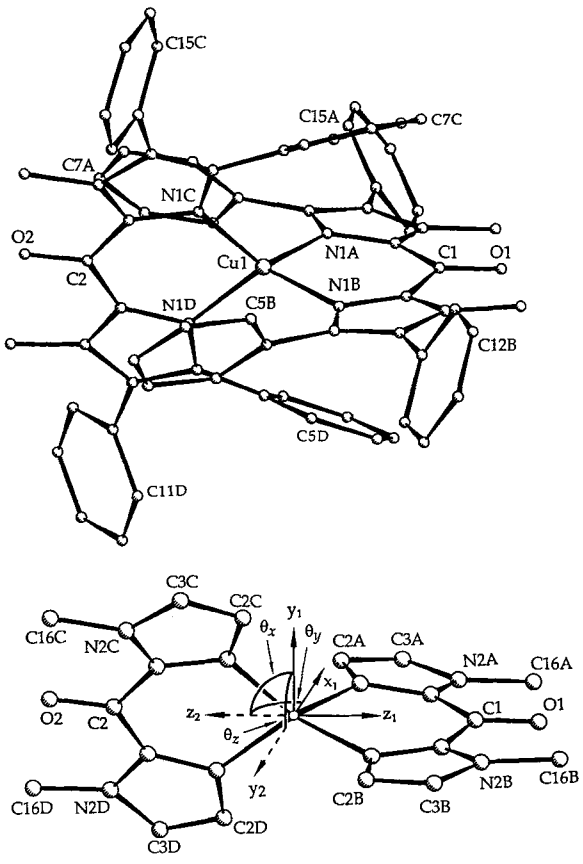

Fig. 4. PLUTO views of the $[Cu(bimdpk)_2]^+$ cation in $[Cu(bimdpk)_2][PF_6]$, including phenyl groups (top) and with the phenyl groups removed and showing the axis system to which θ_x, θ_y and θ_z are related (bottom). The orthonormal unit vectors x_1, y_1 and z_1 are chosen so that N1A, Cu and N1B lie in the x_1z_1 plane with z_1 along the bisector of angle N1A-Cu-N1B. The unit vector z_2 lies along the bisector of N1C-Cu-N1D. The unit vector y_2 is defined as being perpendicular to the N1C/Cu/N1D plane. θ_x is the angle between z_2 and y_1, θ_y between z_2 and x_1 and θ_z between y_2 and y_1. The latter defines the dihedral angle between intraligand CuN_2 planes.

Table 3. Selected bond lengths (Å), bond angles (°), distortion angles (°) and average dihedral angles (°) for $[Cu(bimdpk)_2][BF_4]_2$, $[Cu(bimdpk)_2][PF_6]$ and Cu^{II}–Zn^{II} superoxide dismutase (e.s.d.'s in parentheses).

	$[Cu(bimdpk)_2][BF_4]_2$	$[Cu(bimdpk)_2][PF_6]$	$Cu^{II}ZnSOD$ [4]	$Cu^{I}ZnSOD$ [13] Subunit A
Bond lengths in coordination sphere				
Cu1–N1	1.968(6)			
Cu1–N1A	1.968(6)			
Cu1–N3	1.934(6)			
Cu1–N3A	1.934(6)			
Cu1–N1A		2.009(6)		
Cu1–N1B		1.993(6)		
Cu1–N1C		1.989(6)		
Cu1–N1D		2.004(6)		
Cu–His44			2.01	2.16
Cu–His46			2.11	2.21
Cu–His118			2.10	2.19
Cu–His61			2.21	2.31
Bond angles in coordination sphere				
N1-Cu1-N1A	95.6(4)			
N1-Cu1-N3	131.5(3)			
N1-Cu1-N3A	105.4(3)			
N1A-Cu1-N3	105.4(3)			
N1A-Cu1-N3A	131.5(3)			
N3-Cu1-N3A	92.7(3)			
N1A-Cu1-N1B		93.7(3)		
N1A-Cu1-N1C		129.3(2)		
N1A-Cu1-N1D		107.5(2)		
N1B-Cu1-N1C		109.9(2)		
N1B-Cu1-N1D		124.8(3)		
N1C-Cu1-N1D		95.0(2)		
His44-Cu-His46			130.2	142.5
His44-Cu-His118			93.8	97.4
His44-Cu-His61			74.7	85.4
His46-Cu-His118			106.4	104.0
His46-Cu-His61			89.1	92.8
His118-Cu-His61			164.5	153.3
Distortion angles				
θ_x	90.0	86.8	73.7	82.6
θ_y	90.0	89.3	89.3	84.8
θ_z	68.2	74.9	47.7	48.6
Average dihedral angles [a]				
meim/4-Ph	53.9	56.9		
meim/5-Ph	54.0	44.7		
meim/meim	12.7	13.6		
meim to CuN_2	9.1	13.1		

[a] Meim: *N*-methylimidazole ring plane; Ph: phenyl ring plane.

from the $[Cu(bimdpk)_2]^{2+/+}$ cations (the shortest contact distance from an F atom of the counterion to the periphery of the complex is 2.579 Å in $[Cu(bimdpk)_2][BF_4]_2$ and 2.474 Å in $[Cu(bimdpk)_2][PF_6]$) and do not coordinate to the copper ion. Both structures contain cations with a $[CuN_4]$ geometry that may be described as intermediate between tetrahedral and square planar, possessing approximately D_2 point symmetry and representing a compromise between the normally preferred four-coordinate geometries of Cu^{II} and Cu^{I} complexes. The angles θ_x, θ_y and θ_z, and the intraligand bite angles (Table 3, Figs. 3 and 4) define how these structures deviate from the square-planar and tetrahedral geometrical extremes.[30] The angle θ_z is the interligand dihedral angle, while θ_x and θ_y represent rocking displacements of one ligand with respect to the other.

The rigidity of the BIMDPK ligand confines the N-Cu-N bite angle to an average of $94.2\pm1.4°$ in $[Cu(bimdpk)_2]^{2+}$ and $94.4\pm0.6°$ in $[Cu(bimdpk)_2]^{+}$. The steric bulk of the ligand, through interligand interactions between the phenyl groups substituted at the 4-positions of the imidazole rings, prevents the adoption of a square-planar geometry. These interactions arise primarily from the steric repulsions between the H atoms at the 2-positions of the 4-phenyl rings (contact distances: H13···H34A = 2.50 Å, H13A···H34 = 2.50 Å in $[Cu(bimdpk)_2]^{2+}$ and H9A···H5C = 3.08 Å, H9B···H5D = 2.44 Å in $[Cu(bimdpk)_2]^{+}$; H atom numbering is defined by the C atom number to which it is bonded). Thus, two different facets of the BIMDPK ligand—the bite angle and the steric bulk—lead to bis(diimidazole) copper complexes possessing essentially the same coordination geometry for Cu^{II} and Cu^{I}.

On complexation to Cu^{II} and Cu^{I} the dihedral angle between the two imidazole rings of BIMDPK decreases from 54.9° in the free ligand to an average of 12.7° in $[Cu(bimdpk)_2][BF_4]_2$ and 13.6° in $[Cu(bimdpk)_2][PF_6]$. Thus, in these complexes the imidazole rings of each BIMDPK ligand are almost coplanar. The average dihedral angle between the imidazole plane and the plane containing the 5-phenyl group does not change significantly on complexation; this would be expected since these groups are directed away from the coordination sphere of the $[Cu(bimdpk)_2]^{2+/+}$ complexes (see Figs. 3 and 4). In contrast, the average dihedral angle between the imidazole plane and the plane containing the 4-phenyl group increases on complexation, as the 4-phenyl groups rotate to accommodate the bulk of the other ligand. The average dihedral angle between the imidazole rings of the ligand and their respective CuN_2 planes is 9.1° for $[Cu(bimdpk)_2][BF_4]_2$ and is 13.1° for $[Cu(bimdpk)_2][PF_6]$; that is, in both structures the imidazole groups are approximately coplanar with their CuN_2 planes.

0947-6539/96/0206-0688 $ 15.00+.25/0 Chem. Eur. J. 1996, 2, No. 6

There are no appreciable changes in the ligand intramolecular bond lengths and angles on complexation to Cu^{II} or Cu^{I}, except for the angle C2-C33-C18, which describes the geometry about the ligand carbonyl bridge. In $[Cu(bimdpk)_2]^{2+}$ (C2-C1-C2 = 121(1)° and C19-C18-C19 = 118(1)°) and in $[Cu(bimdpk)_2]^{+}$ (C1A-C1-C1B = 120.3(7)° and C1C-C2-C1D = 121.2(7)°) this angle is greater than in the free ligand (C2-C33-C18 = 115.5(4)°).

The Cu^{II}–N and Cu^{I}–N distances in the $[Cu(bimdpk)_2]^{2+/+}$ cations are typical of those observed in other Cu^{II}–bis(diimidazole) complexes[17, 19] and Cu^{I} tetrakisimidazole complexes,[19, 31] respectively. The average difference in the Cu–N bond lengths (Δ) between the two oxidation states of $[Cu(bimdpk)_2]^{2+/+}$ is 0.050 Å, slightly less than that observed for $[Cu^{II,I}((imid)_2bp)_2][BF_4]_{2,1}$ (Δ = 0.083 Å)[19] and significantly less than the differences observed for the five-coordinate complexes $[Cu^{II,I}(imidH)_2DAP][BF_4]_{2,1}$ (Δ = 0.220 Å) and $[Cu^{II,I}(py)_2DAP][BF_4]_{2,1}$ (Δ = 0.140 Å)[32] [(imidH)$_2$DAP: bis-2,6-[1-((2-imidazol-4-ylethyl)imino)ethyl]pyridine; (py)$_2$DAP: bis-2,6-[1-((2-pyridin-2-ylethyl)imino)ethyl]pyridine]; (imid)$_2$bp: 2,2′-bis[2-imidazolyl]biphenyl). The average difference in the intraligand bond angles for $[Cu(bimdpk)_2]^{2+/+}$ is around 1° and is considerably smaller than for the related $[Cu((imid)_2bp)_2]^{2+/+}$ system (21.3°).[19] The pattern of Cu–N bond lengths, intraligand angles, dihedral angles, together with the values of the angles θ_x, θ_y and θ_z for $[Cu(bimdpk)_2]^{2+}$ and $[Cu(bimdpk)_2]^{+}$ (Table 3) indicate that there are only small differences in the geometry about these Cu^{II} and Cu^{I} centres. In the comparable pair of copper centres $[Cu((imid)_2bp)_2][BF_4]_2$ and $[Cu((imid)_2bp)_2][BF_4]$, θ_z (θ_z = 86.3 and 88.0°, respectively) are close to the ideal tetrahedral value,[19] whereas in $[Cu(bimdpk)_2]^{2+}$ and $[Cu(bimdpk)_2]^{+}$ (θ_z = 68.2 and 74.9°, respectively) θ_z indicates geometries that are displaced from a regular tetrahedron towards a square-planar geometry. However, the average intraligand dihedral angle for $[Cu((imid)_2bp)_2]^{2+}$ (141.9°) indicates a greater distortion towards a square-planar geometry than in $[Cu(bimdpk)_2]^{2+}$ (94.2 ± 1.4°).

Electronic Properties: The X-band EPR spectra (77 K) of $[Cu(bimdpk)_2][BF_4]_2$ recorded on the powder, a MeCN/toluene solution and a CH_2Cl_2/toluene solution are typical of a rhombic D_2 $Cu^{II}N_4$ centre possessing a d_{xy} ground state.[33] All the spectra show a resolved metal hyperfine interaction (Table 4) that is considerably smaller than from those of other tetrakisimidazole complexes (A_z = 130–180 × 10^{-4} cm^{-1}),[16–18] including $[Cu((imid)_2bp)_2][BF_4]_2$ for which A_z = 130 × 10^{-4} cm^{-1}.[19] A correlation of θ_z with A_z indicates that as θ_z increases A_z decreases.[34] On this basis it seems surprising that $[Cu((imid)_2bp)_2][BF_4]_2$ (θ_z = 86.3°) has a greater A_z than $[Cu(bimdpk)_2][BF_4]_2$ (θ_z = 68.2°). However, the θ_z/A_z correlation takes no account of the intraligand angles, which are substantially different in $[Cu(bimdpk)_2]^{2+}$ (94.2 ± 1.4°) and $[Cu((imid)_2bp)_2]^{2+}$ (141.9°); clearly, this will affect the electronic structure of the Cu^{II} centre. Also, it should be noted that the π-acceptor properties of BIMDPK in $[Cu(bimdpk)_2][BF_4]_2$ and overlap with the d_{xy} orbital may be sufficient to delocalise some of the electron density off the metal and onto the ligands thereby lowering A_z. Concordant with the low A_z for $[Cu(bimdpk)_2][BF_4]_2$, g_z (Table 4) is elevated over those for other bis(diimidazole)-copper(II) systems (g_z = 2.26–2.27).[16, 17]

Table 4. EPR parameters for $[Cu(bimdpk)_2][BF_4]_2$ recorded at 77 K and X-band frequency.

	g_x	g_y	g_z	$A_z/10^{-4}$ cm^{-1}
MeCN/10% toluene	2.080	2.080	2.301	121.0
CH_2Cl_2/10% toluene	2.077	2.077	2.292	113.8
powder	2.080	2.075	2.291	112.3

The EPR spectra of the powder and of the MeCN/toluene and CH_2Cl_2/toluene frozen solutions closely resemble one another (Table 4); this indicates that the solid-state structure of $[Cu(bimdpk)_2]^{2+}$ is essentially conserved in solution. The fact that A_z value in MeCN differs from that in CH_2Cl_2 and in the solid state implies some solvation of the cation, perhaps leading to a minor perturbation of the CuN_4 coordination sphere.

The UV/vis data recorded for the ligand BIMDPK and its Cu^{II} and Cu^{I} complexes are presented in Table 5. BIMDPK exhibits strong absorptions at energies of around 38200 and 27100 cm^{-1}, which may be attributed to $\pi \rightarrow \pi^*$ transitions. $[Cu(bimdpk)_2][BF_4]_2$ exhibits absorptions between approximately 43000 and 13000 cm^{-1} of comparable energy and intensity to other copper(II)–imidazole systems.[16–19] The absorptions at around 42400 and 25800 cm^{-1} are attributed to ligand-based $\pi \rightarrow \pi^*$ transitions with an underlying ligand-to-metal charge transfer (LMCT) transition in the 25800 cm^{-1} absorption. The 25800 cm^{-1} $\pi \rightarrow Cu^{II}$ LMCT band is red-shifted by 1000–5000 cm^{-1} from the lowest energy $\pi \rightarrow Cu^{II}$ LMCT band for tetrakis (alkylated monoimidazole) Cu^{II} complexes.[18] Interactions between the π orbitals on the imidazole rings through the carbonyl bridge in BIMDPK would be expected to raise the energies of the imidazole frontier orbitals thus lowering the energy of $\pi \rightarrow Cu^{II}$ LMCT. Red shifts of a comparable magnitude for the corresponding absorptions in $[Cu((imid)_2bp)_2][BF_4]_2$[19] and bis(4,4′,5,5′-tetramethyl-2,2′-biimidazole)copper(II) dinitrate[17] have been attributed to similar electronic interactions. In the absorption spectrum of $[Cu(bimdpk)_2][BF_4]_2$

Table 5. Summary of electronic absorption spectra with band assignments for $[Cu(bimdpk)_2][BF_4]_2$ and $[Cu(bimdpk)_2][PF_6]$ (LF = ligand field; CT = charge transfer).

	λ/nm	$\tilde{\nu}$/cm^{-1}	ε/M^{-1}cm^{-1}	Assignment
BIMDPK	369	27100	20000	$\pi \rightarrow \pi^*$
in MeCN	262	38200	22000	$\pi \rightarrow \pi^*$
BIMDPK	375	27000	40000	$\pi \rightarrow \pi^*$
in CH_2Cl_2	262	38200	40000	$\pi \rightarrow \pi^*$
$[Cu(bimdpk)_2][BF_4]_2$	739	13500	497	LF
in MeCN	387	25800	37000	$\pi \rightarrow \pi^*/\pi \rightarrow Cu^{II}$ CT
	236	42400	38000	$\pi \rightarrow \pi^*/n \rightarrow Cu^{II}$ CT
$[Cu(bimdpk)_2][BF_4]_2$	750	13300	570	LF
in CH_2Cl_2	394	25400	46000	$\pi \rightarrow \pi^*/\pi \rightarrow Cu^{II}$ CT
	246	40700	50000	$\pi \rightarrow \pi^*/n \rightarrow Cu^{II}$ CT
$[Cu(bimdpk)_2][BF_4]_2$	687	14600	–	LF
mull [a]	429	23300	–	$\pi \rightarrow \pi^*/\pi \rightarrow Cu^{II}$ CT
$[Cu(bimdpk)_2][PF_6]$	640	15600	252	$Cu^{I} \rightarrow \pi^*$ CT
in MeCN	381	26200	45000	$Cu^{I} \rightarrow \pi^*$ CT
	270	37000	37000	$\pi \rightarrow \pi^*$
$[Cu(bimdpk)_2][PF_6]$	640	15600	260	$Cu^{I} \rightarrow \pi^*$ CT
in CH_2Cl_2	389	25700	48000	$Cu^{I} \rightarrow \pi^*$ CT
$[Cu(bimdpk)_2][PF_6]$	639	15700	–	$Cu^{I} \rightarrow \pi^*$ CT
mull [a]	423	23600	–	$Cu^{I} \rightarrow \pi^*$ CT

[a] Poly(dimethylsiloxane) mull.

a band of considerably lower intensity at approximately 13500 cm^{-1} lies outside the range of other Cu^{II}–imidazole LM-CT transitions and, on the basis of comparisons with other distorted tetrahedral $[Cu^{II}N_4]$ chromophores,[19, 35, 36] has been assigned to ligand-field d–d transitions to the d_{xy} orbital. This absorption gives rise to the emerald green colour of this compound. The deep blue colour of $[Cu(bimdpk)_2][PF_6]$ arises from the absorption at 15600 cm^{-1}, which is assigned to MLCT; this occurs at a similar wavenumber and extinction coefficient to other four-coordinate Cu^{I} complexes with N π-acceptor ligands.[37] The bands at around 26000, 37000 (MeCN) and 44000 (CH_2Cl_2) cm^{-1} are assigned to ligand-based $\pi \rightarrow \pi^*$ transitions by comparison with the UV/vis spectrum of the free ligand. The solid-state UV/vis spectrum of $[Cu(bimdpk)_2][PF_6]$ shows similar features to the solution spectra. Thus, the UV/vis and EPR spectra indicate that the solid-state structures of $[Cu(bimdpk)_2]^{2+}$ and $[Cu(bimdpk)_2]^{+}$ are essentially conserved in solutions in donor (MeCN) and nondonor (CH_2Cl_2) solvents.

Electron Transfer: Cyclic voltammetry was carried out on 1 mM solutions of $[Cu(bimdpk)_2][BF_4]_2$ and $[Cu(bimdpk)_2][PF_6]$ in a 0.2 M solution of $[NnBu_4][BF_4]$ in MeCN (Fig. 5), a medium

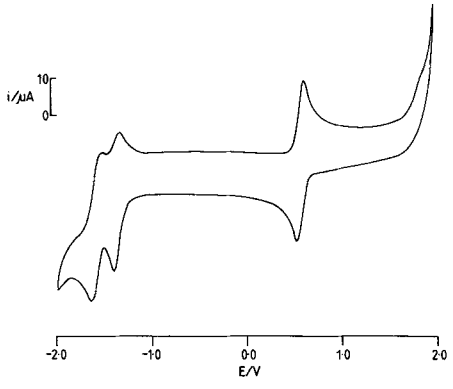

Fig. 5. Cyclic voltammogram of a 1 mM solution of $[Cu(bimdpk)_2][BF_4]_2$ recorded at 298 and 253 K in a 0.2 M solution of $[NnBu_4][BF_4]$ in MeCN using a glassy carbon electrode, a scan rate of 100 mVs^{-1} and an SCE reference electrode.

which gave UV/vis and EPR spectra identical to those recorded in MeCN alone. Both complexes possess identical cyclic voltammograms over the potential range −2.0 to +2.0 V, clearly showing evidence for three processes, which were subsequently investigated separately and found to be independent of one another. The lowest potential wave at −1.59 V (vs. SCE) is assigned to ligand-based redox on the basis of comparisons with the redox chemistry of the ligand alone. The wave at −1.37 V (vs. SCE) has been tentatively assigned to a ligand-based redox process that occurs in the presence of copper. Stirred voltammetry and controlled potential electrolysis and subsequent UV/vis and EPR spectroscopic studies showed that the process at +0.59 V (vs. SCE) can be unambiguously assigned to the Cu^{II}/Cu^{I} redox process. In the less polar solvent, CH_2Cl_2, the redox reaction occurs at $E_{1/2} = +0.80$ V (vs. SCE). In both solvents, MeCN and CH_2Cl_2, the linear relationship between i_p^c and $v^{1/2}$, the independence with scan rate of the difference between the oxidative and reductive peak potentials, and the ratio $i_p^c/i_p^a = 1$ (Table 6) indicate that the Cu^{II}/Cu^{I} couple is electrochemically reversible over the potential scan rate range of 50–300 mVs^{-1}. This reversibility is not unexpected given the similarity of copper coordination geometries in $[Cu(bimdpk)_2][BF_4]_2$ and $[Cu(bimdpk)_2][PF_6]$. A solution of $[Cu(bimdpk)_2][BF_4]_2$ in MeCN can be chemically reduced by treatment with a stoichiometric amount of Fc. This solution loses its Cu^{II} EPR signal and turns dark blue.

Table 6. Electrochemical data for the Cu^{II}/Cu^{I} couple recorded in 0.2 M $[NnBu_4][BF_4]$ solutions in CH_2Cl_2 and MeCN at 293 K and at a scan rate of 100 mVs^{-1}.

	E/V vs. SCE	i_p^c/i_p^a	$E_p^c - E_p^a$/mV	Solvent
$[Cu(bimdpk)_2][BF_4]_2$	0.59	1.00	70	MeCN
$[Cu(bimdpk)_2][PF_6]$	0.59	1.00	70	MeCN
ferrocene	0.43	1.00	70	MeCN
$[Cu(bimdpk)_2][BF_4]_2$	0.80	1.00	80	CH_2Cl_2
$[Cu(bimdpk)_2][PF_6]$	0.80	1.01	80	CH_2Cl_2
ferrocene	0.52	1.00	70	CH_2Cl_2

Examples of reversible or quasi-reversible Cu^{II}/Cu^{I} redox couples with equivalent ligation in the oxidised and reduced forms are rare. They include $[Cu^{II,I}((imidH)_2DAP)][BF_4]_{2,1}$ and $[Cu^{II,I}((py)_2DAP)][BF_4]_{2,1}$ ($E_{1/2} = -0.27$ V in MeCN vs. SCE and −0.14 V in MeCN vs. SCE, respectively)[20] and $[Cu^{II,I}((imid)_2bp)_2][BF_4]_{2,1}$ ($E_{1/2} = +0.11$ V in MeCN vs. SCE).[19] The $E_{1/2}$ value for the $[Cu(bimdpk)_2]^{2+/+}$ couple at +0.59 V in MeCN (vs. SCE) is considerably more positive than those of other $CuN_{4,5}$ complexes. One factor that may be important in this respect is the π-acceptor characteristics of BIMDPK, which may stabilise the Cu^{I} state; the intense MLCT absorption at 15600 cm^{-1} of $[Cu(bimdpk)_2][PF_6]$ suggests that there are suitable low-energy unoccupied ligand-based acceptor orbitals.

The electron self-exchange constant, k, for the $[Cu(bimdpk)_2]^{2+/+}$ couple has been examined by ^{1}H NMR spectroscopy at 300 MHz at 298 and 253 K, using T_1 spin-lattice relaxation times of the ligand N–Me protons in solutions of $[Cu(bimdpk)_2][PF_6]$ in MeCN containing different concentrations of $[Cu(bimdpk)_2][BF_4]_2$. The value of T_1 for the protons in $[Cu(bimdpk)_2][PF_6]$ varies as $P = [T_1^{-1} - T_{10}^{-1}] = k[Cu^{II}]$, where T_{10} is the spin-lattice relaxation time of a proton in the $[Cu(bimdpk)_2]^{+}$ complex.[38, 39] A plot of P versus $[Cu^{II}]$ (Fig. 6), gives $k \leq 1.9 \pm 0.2 \times 10^4$ $M^{-1}s^{-1}$ in CD_3CN at 298 K. This analysis is only valid in the slow exchange limit where $k[T] \ll T_1^{-1}$, where [T] is the total copper concentration in solution.[38–40] A diagnostic test for this condition is to examine how the gradient of a P versus $[Cu^{II}]$ plot varies with temper-

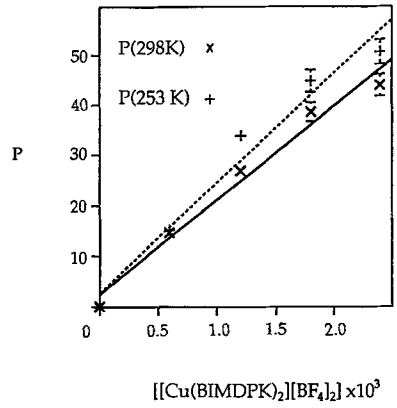

Fig. 6. Plot of $P = [T_1^{-1} - T_{10}^{-1}]$ for the imidazole N–Me proton NMR signal of $[Cu(bimdpk)_2][PF_6]$ at 298 and 253 K in CD_3CN vs. concentration of $[Cu(bimdpk)_2][BF_4]_2$ added, where T_{10} is the spin-lattice relaxation time for the N–Me protons in $[Cu(bimdpk)_2][PF_6]$ in the absence of $[Cu(bimdpk)_2][BF_4]_2$ and T_1 is the spin-lattice relaxation time for the N-Me protons in $[Cu(bimdpk)_2][PF_6]$ as $[Cu(bimdpk)_2][BF_4]_2$ is added at 298 and 253 K.

0947-6539/96/0206-0690 $ 15.00+.25/0 Chem. Eur. J. 1996, 2, No. 6

ature. Figure 6 reveals a temperature-dependent gradient for $[Cu(bimdpk)_2]^{2+/+}$ indicative of a slow exchange limit. The value for the self-exchange rate constant of $[Cu(bimdpk)_2]^{2+/+}$ is comparable to that for $[Cu^{II,I}((1\text{-imidH})_2DAP)][BF_4]_{2,1}$ ($k \leq 1.31 \times 10^4\,M^{-1}s^{-1}$, MeCN)[21] $[Cu^{II,I}(imidH)_2DAP]$ and $[Cu^{II,I}((py)_2DAP)][BF_4]_{2,1}$ ($k \leq 1.76 \times 10^4\,M^{-1}s^{-1}$, MeCN),[20] but greater by a factor of about 10^2 than the value for the related system $[Cu^{II,I}((1\text{-meimid})_2bp)_2][BF_4]_{2,1}$ ($k < 1 \times 10^2\,M^{-1}s^{-1}$, MeCN) ($(1\text{-meimid}_2)_2bp$ = 2,2′-bis[2-(1-methylimidazoyl]biphenyl).[19] It has been suggested that in $[Cu^{II,I}((imid)_2bp)_2]^{2+}$,[19] the orbital containing the unpaired electron lies between the ligands and does not overlap effectively with the ligand orbitals thereby attenuating the rate of electron transfer. In $[Cu(bimdpk_2)]^{2+}$, the EPR spectrum indicates a d_{xy} ground state, and the significant distortion away from a $[CuN_4]$ tetrahedron ($\theta_z = 68.2°$) may result in a greater ligand–d_{xy} orbital overlap with a resultant increase in k.

Discussion

The establishment of a $[Cu^{II}(imidazole)_4]$ core for the two complexes discussed above prompts comparison with the Cu^{II} and Cu^{I} centres of CuZnSOD. Comparison of the parameters in Table 3 shows that, while the bond lengths in $[Cu(bimdpk)_2][BF_4]_2$ and Cu^{II}ZnSOD are similar, θ_x, θ_y and θ_z for $[Cu(bimdpk)_2]^{2+}$ and Cu^{II}ZnSOD describe different distortions from a square-planar geometry. The geometry of $[Cu(bimdpk)_2]^{2+}$ has been described earlier, and for the Cu^{II} centre of Cu^{II}ZnSOD the His 44 ligand lies out of the CuN_3 plane of the other ligands. Cu^{I}ZnSOD possesses an approximately tetrahedral Cu^{I} site in subunit A and a distorted trigonal bipyramidal structure in subunit B.[13] In both subunits the imidazolate bridge is maintained. In addition to the four histidinyl residues in subunit B, a water molecule completes the coordination to Cu^{I}. Comparison between θ_x, θ_y and θ_z for Cu^{I}ZnSOD and $[Cu(bimdpk)_2]^{+}$ reveals that the coordination sphere of $[Cu(bimdpk)_2]^{+}$ involves a smaller distortion from a tetrahedral geometry than that of the subunit A Cu^{I} site in Cu^{I}ZnSOD.

The EPR spectrum of the distorted CuN_4O chromophore in Cu^{II}ZnSOD is anisotropic with $g_x = 2.03$, $g_y = 2.09$, $g_z = 2.26$ and $A_z = 142 \times 10^{-4}\,cm^{-1}$,[41] parameters clearly distinct from those of $[Cu(bimdpk)_2][BF_4]_2$ (Table 4); this reflects the different geometries of the Cu^{II} coordination sphere and the coordination of a water molecule to the Cu^{II} ion. The EPR parameters of $[Cu(bimdpk)_2][BF_4]_2$ approach those of Cu^{II} substituted into the "Zn^{II}" site in $AgCu^{II}SOD$ ($g_x = 2.01$, $g_y = 2.118$, $g_z = 2.316$ and $A_z = 116 \times 10^{-4}\,cm^{-1}$), for which a tetrahedrally distorted N_3O site has been proposed.[42]

The absorption at $25\,800\,cm^{-1}$ in the UV/vis spectrum of $[Cu(bimdpk)_2][BF_4]_2$ is comparable in energy to the lowest energy $\pi(ImH) \rightarrow Cu^{II}$ LMCT transition, which occurs at $26\,500\,cm^{-1}$, for Cu^{II} doped into the pseudotetrahedral "Zn^{II}" site of the system $AgCu^{II}SOD$.[42] The corresponding absorption for Cu^{II} in the native protein occurs at a higher energy ($29\,500\,cm^{-1}$). The maximum of the ligand-field absorption band for $[Cu(bimdpk)_2][BF_4]_2$ lies within the range of such absorptions of Cu^{II}ZnSOD ($18\,000-13\,000\,cm^{-1}$),[42] but blue-shifted from those of Cu^{II} doped into the pseudotetrahedral "Zn^{II}" site in $AgCu^{II}SOD$ ($12\,000-8\,000\,cm^{-1}$).[42]

For low concentrations of O_2^- (slow turnover rate) the mechanism of catalysis by CuZnSOD has been proposed to occur through a two-step mechanism [Eqs. (a) and (b)].[43–46] The

$$Cu^{II}\text{–Im–}Zn^{II} + H^+ + O_2^- \longrightarrow Cu^{I}\,HIm\text{–}Zn^{II} + O_2 \quad (a)$$

$$Cu^{I}\,HIm\text{–}Zn^{II} + H^+ + O_2^- \longrightarrow Cu^{II}\text{–Im–}Zn^{II} + H_2O_2 \quad (b)$$

results of EXAFS,[15] UV[43] and NMR[14, 47] spectroscopic investigations support the protonation and breaking of the imidazolate bridge in the first step to form a three-coordinate Cu^{I} site. During the second step the imidazolate bridge is reformed when O_2^- oxidises Cu^{I}ZnSOD to Cu^{II}ZnSOD. The protons necessary for this step are provided by the imidazole of His 61 and deprotonation allows the imidazolate bridge to reform. However, under saturating conditions the turnover rate of $10^6\,M^{-1}s^{-1}$ is not consistent with this mechanism, since it involves several bond-breaking and bond-making steps.[48] An alternative mechanism has been proposed where the imidazolate bridge remains intact, and there is little change in coordination geometry at the Cu centre from Cu^{II}ZnSOD to Cu^{I}ZnSOD and vice versa during turnover.[49] This mechanism is supported by the crystal structure of Cu^{I}ZnSOD,[13] which shows that the imidazolate bridge is conserved at the Cu^{I} site and that the centre in subunit A is almost isostructural with the Cu^{II} site in Cu^{II}ZnSOD.[4]

A requirement for CuZnSOD to be a successful catalyst in steps (a) and (b) is for the redox potential of the Cu^{II}/Cu^{I} couple to lie in between the reported[50] values of $E(O_2/O_2^-) = -0.16$ V (at pH = 7, vs. NHE(H_2O)) and $E(O_2^-; 2H^+/H_2O_2) = 0.89$ V (at pH = 7, vs. NHE(H_2O)). A reduction potential for the Cu^{II} centre of CuZnSOD of 0.403 V (at pH = 7, vs. NHE(H_2O)) has been obtained by spectroelectrochemistry[51] and a value of 0.32 V (at pH = 7.4, vs. NHE(H_2O)) by cyclic voltammetry, and the potential was found to be pH dependant over the range pH = 5–9;[52] titrations with $K_3[Fe(CN)_6]$ and $K_2[IrCl_6]$ place E at 0.40 V and 0.20 V vs. NHE(H_2O), respectively.[53, 54]

Cofre and Sawyer considered the redox chemistry of H_2O_2 in anhydrous MeCN and in the presence of picolinate anion,[50] which was assumed to provide a proton sink, and they reported the following redox potentials vs. SCE: $E(O_2, H^+/HO_2) = -0.2$ V and $E(HO_2, H^+/H_2O_2) = +0.8$ V. The reduction potential of $[Cu(bimdpk)_2]^{2+/+}$ in MeCN vs. SCE ($E = 0.59$ V) lies between these two values. Thus, thermodynamically, $[Cu(bimdpk)_2]^{2+}$ should be reduced by superoxide and $[Cu(bimdpk)_2]^{+}$ should be oxidised by superoxide. Treatment of a solution of $[Cu(bimdpk)_2][BF_4]_2$ in MeCN with a stoichiometric amount of KO_2 solubilised in MeCN by [18]crown-6 resulted in reduction to $[Cu(bimdpk)_2]^{+}$; the solution lost its EPR signal and possessed a UV/vis absorption spectrum identical to that of $[Cu(bimdpk)_2][PF_6]$. However, no evidence for the oxidation of $[Cu(bimdpk)_2][PF_6]$ in MeCN occurred when the solution was treated with KO_2 solubilised in MeCN by [18]crown-6 and then acidified by trifluoroacetic acid. A possible explanation for the failure of the latter process is that, although thermodynamically favourable, oxidation of $[Cu(bimdpk)_2]^{+}$ by superoxide does not occur at a rate competitive with superoxide disproportionation under these conditions.[55] Thus, for reduction, superoxide must initially be coordinated to copper and the steric bulk of the ligands may restrict access. In contrast to this inner-sphere mechanism, the redox between $[Cu(bimdpk)_2]^{2+}$ and superoxide could be an outer-sphere process. An alternative mechanism for superoxide dismutation by CuZnSOD has been proposed involving a Cu^{2+}–O_2^- intermediate stabilised through a hydrogen bond from the distal O of the coordinated O_2^- and the amino acid Arg 141.[56–58] This intermediate is then reduced by a second O_2^- ion before being protonated by solvent protons. It has been suggested that this mechanism should be reconsidered, in the light of recent X-ray crystallographic results,[13] to be operating

when CuZnSOD is under saturating conditions. It appears that, in the reaction of $[Cu(bimdpk)_2][BF_4]_2$ with superoxide, this mechanistic pathway is not available due to the steric hindrance of the ligands preventing access to the metal and, therefore, a means of stabilising O_2^- as a $Cu^{II}-O_2^-$ intermediate.

Type I copper proteins exhibit a wide range of reduction potentials from 180 mV vs. NHE for stellacyanin[59] to 680 mV at pH = 2 vs. NHE(H_2O) for rusticyanin[60, 61] with most, including the plastocyanins ($E \approx 380$ mV vs. NHE(H_2O)),[62-64] operating around 280–380 mV.[65] In order to relate the potential of the $[Cu(bimdpk)_2]^{2+/+}$ couple in MeCN ($E = 0.56$ V vs. NHE(H_2O)) to Type I copper proteins, effects due to the protein/water environment must be considered. While numerous effects contribute to the reduction potentials of proteins,[66] including entropy terms,[67] the effects due to the dielectric constant of the medium can be evaluated by using the Born equation [Eq. (1)],[68-70] where ΔG°_{solv} (kJ mol^{-1}) is the Gibbs

$$\Delta G^\circ_{solv} = -\frac{z_i^2 e^2 N_a}{8\pi\varepsilon_0 r_i}\left(1-\frac{1}{\varepsilon_r}\right) \quad (1)$$

free energy associated with transferring an ion of charge z_i and radius r_i from a vacuum into a solvent of relative permittivity ε_r. The difference in Gibbs free energy for the Cu^{II} and Cu^{I} ions is given by Equation (2).

$$\Delta G^\circ_{redox} = -\frac{e^2 N_a}{8\pi\varepsilon_0}\left(\frac{z(Cu^I)^2}{r(Cu^I)}-\frac{z(Cu^{II})^2}{r(Cu^{II})}\right)\left(1-\frac{1}{\varepsilon_r}\right) \quad (2)$$

The difference in ΔG°_{redox} on moving from a solvent of relative permittivity ε_a to one of relative permittivity ε_b may be represented by Equation (3) Thus, the change in redox potential

$$\Delta(\Delta G^\circ_{redox}) = -\frac{e^2 N_a}{8\pi\varepsilon_0}\left(\frac{z(Cu^I)^2}{r(Cu^I)}-\frac{z(Cu^{II})^2}{r(Cu^{II})}\right)\left(\frac{1}{\varepsilon_a}-\frac{1}{\varepsilon_b}\right) \quad (3)$$

ΔE° (V) for the Cu^{II}/Cu^{I} couple on moving from solvent A to solvent B may be approximated by Equation (4).

$$\Delta E^\circ = \frac{e^2 N_a}{8\pi\varepsilon_0 F}\left(\frac{z(Cu^I)^2}{r(Cu^I)}-\frac{z(Cu^{II})^2}{r(Cu^{II})}\right)\left(\frac{1}{\varepsilon_a}-\frac{1}{\varepsilon_b}\right) \quad (4)$$

Estimates of $r(Cu^{II}) = 911.5$ pm and $r(Cu^{I}) = 920.6$ pm may be obtained by measuring the radius of the smallest sphere that encloses the structures of $[Cu(bimdpk)_2]^{2+}$ and $[Cu(bimdpk)_2]^{+}$, respectively, as determined by X-ray crystallography. Thus, on transferring the $[Cu(bimdpk)_2]^{2+/+}$ couple ($E = 0.56$ V vs. NHE(H_2O)) from MeCN ($\varepsilon_a = 37.5$) to a protein/water environment ($\varepsilon_b \approx 10$[71]), E for this couple is raised to approximately 0.73 V vs. NHE(H_2O). This estimated potential is 350 mV higher than that for most Type I centres, suggesting that there are some aspects of the copper coordination sphere of Type I centres that stabilise Cu^{II} to a greater extent than in $[Cu(bimdpk)_2]^{2+}$. This stabilisation may arise from charge donation by the Cys–S thiolate ligand, which is at an unusually short distance and contains high covalency.[71] This covalency is also believed to be responsible for the unusually small hyperfine splitting ($A_{\|} < 90 \times 10^{-4}$ cm^{-1}) that is observed in the X-band EPR spectra for these proteins.[72] In addition to this charge donation, increased stabilisation of the Cu^{II} site may arise from the differences in geometry at the active site of Type I centres and $[Cu(bimdpk)_2]^{2+}$. While the unusually long MetS–Cu bond results in a only a small interaction with the metal, it has been suggested that this forces an axial Jahn–Teller distortion, lowering the symmetry of the copper centre to C_s and trapping the oxidised form of the protein in a Jahn–Teller minimum.[71] The tetragonal distortion is more common amongst copper(II) compounds, but in the case of $[Cu(bimdpk)_2]^{2+}$ intraligand steric interactions limit its degree, destabilising $[Cu(bimdpk)_2]^{2+}$ and raising the potential of the $[Cu(bimdpk)_2]^{2+/+}$ couple.

The values of electron self-exchange rate for several Type I copper proteins have been determined. These include stellacyanin (*Rhus vernicifera*, 1.2×10^5 M^{-1} s^{-1}),[73] azurin (*Pseudomonas aeruginosa*, 9.6×10^5 M^{-1} s^{-1}),[74] azurin (*Alcaligenes denitrificans*, 4.0×10^5 M^{-1} s^{-1}),[75] amicyanin (*Thiobacillus versutus*, 1.3×10^5 M^{-1} s^{-1}),[76] plastocyanin (*Anabaena variabilis*, 3.2×10^5 M^{-1} s^{-1})[38] and plastocyanin (parsley, 3.3×10^3 M^{-1} s^{-1}).[77] While k for $[Cu(bimdpk)_2]^{2+/+}$ (1.9×10^4 M^{-1} s^{-1}) is comparable to that for plastocyanin (parsley), it is two orders of magnitude below that of the other Type I proteins. In $[Cu(bimdpk)_2]^{2+/+}$, azurin[10] and plastocyanin[9] the oxidised and reduced forms are nearly isostructural. Thus, these sites would be subject to a small inner-sphere reorganisational Franck–Condon barrier for the Cu^{II}/Cu^{I} redox couple, which would promote facile electron transfer. An Eyring plot[40] of k over the temperature range 253–298 K yields approximate values for the enthalpy of activation $\Delta H^\ddagger = -4 \pm 3$ kJ mol^{-1} and the entropy of activation $\Delta S^\ddagger = -177 \pm 9$ J K^{-1} mol^{-1}. The small value of $\Delta H^\ddagger$ is not unexpected given the similarity of the geometries of the $[Cu(bimdpk)_2]^{2+}$ and $[Cu(bimdpk)_2]^{+}$ cations. The value of $\Delta S^\ddagger$ for $[Cu(bimdpk)_2]^{2+/+}$ is similar in magnitude to other Cu^{II}/Cu^{I} complexes ($\Delta S^\ddagger = -103$ J K^{-1} mol^{-1}[32, 78, 79]). The electron self-exchange for azurin, $\Delta S^\ddagger = +96$ J mol^{-1} K^{-1},[80] which favours rapid electron transfer, is significantly greater than that for $[Cu(bimdpk)_2]^{2+/+}$ and other Cu^{II}/Cu^{I} coordination complexes.[32] The positive entropy of activation is believed to be associated with the release of ordered water molecules, which are discharged when two azurin molecules associate through their hydrophobic patches prior to electron self-exchange.[81] A similar mechanism is also believed to be active in amicyanin ($\Delta S^\ddagger = +26$ J mol^{-1} K^{-1})[77] and plastocyanin.[38] In the case of plastocyanin (parsley), the electron self-exchange rate is attenuated by the negative charge associated with the protein; the reduced protein has an estimated charge of -9 ± 1 (pH = 7) compared to +1 (pH = 7) for *A. variabilis* plastocyanin.[38, 82] Such effects promoting electron self-exchange are absent in $[Cu(bimdpk)_2]^{2+/+}$ and other complexes.[32]

Conclusions

The new, sterically hindered, diimidazole ligand BIMDPK has been synthesised, characterised and shown to form the complexes $[Cu(bimdpk)_2]^{2+}$ and $[Cu(bimdpk)_2]^{+}$ with essentially the same CuN_4 coordination geometry. This stereochemistry at the metal centre is controlled by the nature of the intraligand geometry and the interligand interactions. The properties of these centres demonstrate that it is possible to achieve a Cu^{II} centre with an EPR spectrum possessing a low A_z value and a reversible Cu^{II}/Cu^{I} redox couple with a high potential and fast self-exchange rate through the maintenance of a tetrahedral geometry for a $[Cu(imidazole)_4]$ coordination sphere. Therefore, the possibility of $[Cu(histidine)_4]$ centres involved in biological electron transfer should not be precluded.

Acknowledgements: We gratefully acknowledge the EPSRC for the provision of a studentship (J. M.), the Royal Society for financial support (D. C.), the assistance of Dr. G. A. Morris and J. Friend in the NMR self-exchange measurements, and valuable discussions with Dr. T. C. Higgs and R. Bhalla. We thank a referee for helpful and insightful comments concerning the electrochemistry.

Received: September 22, 1995 [F217]

[1] J. P. Glusker, *Adv. Protein Chem.* **1991**, *42*, 1.
[2] P. M. Coleman, H. C. Freeman, J. M. Guss, M. Murata, V. A. Norris, J. A. M. Ramshaw, M. P. Venkatappa, *Nature* **1978**, *272*, 319.
[3] E. T. Adman, R. E. Stenkamp, L. C. Sieker, L. H. Jensen, *J. Mol. Biol.* **1978**, *123*, 35.
[4] J. A. Tainer, E. D. Getzoff, K. M. Beem, J. S. Richardson, D. C. Richardson, *J. Mol. Biol.* **1982**, *160*, 181.
[5] N. Ito, S. E. V. Phillips, C. Stevens, Z. B. Ogel, M. J. McPherson, J. N. Keen, K. D. S. Yadav, P. F. Knowles, *Nature* **1991**, *350*, 87.
[6] B. Linzen, N. M. Soeter, A. F. Riggs, H. J. Schneider, W. Schartau, M. D. Moore, E. Yokota, P. Q. Behrens, H. Nakashima, T. Takagi, T. Nemoto, J. M. Verijken, H. J. Bak, J. J. Beintema, A. Volbeda, W. P. J. Gaykema, W. G. J. Hol, *Science* **1985**, *229*, 519.
[7] J. W. Godden, S. Turley, D. C. Teller, E. T. Adman, M. Y. Liu, W. J. Payne, J. LeGall, *Science* **1991**, *253*, 438.
[8] A. Messerschmidt, A. Rossi, R. Ladenstein, R. Huber, M. Bolognesi, G. Gatti, A. Marchesini, R. Petruzzelli, A. Finazzi-Agro, *J. Mol. Biol.* **1989**, *206*, 513.
[9] J. M. Guss, P. R. Harrowell, M. Murata, V. A. Norris, H. C. Freeman, *J. Mol. Biol.* **1986**, *192*, 361.
[10] W. E. B. Shepard, B. F. Anderson, D. A. Lewandoski, G. E. Norris, E. N. Baker, *J. Am. Chem. Soc.* **1990**, *112*, 7817.
[11] J. A. Fee, B. P. Gaber, *J. Biol. Chem.* **1972**, *247*, 60.
[12] N. Boden, M. C. Holmes, P. F. Knowles, *Biochem. J.* **1979**, *177*, 303.
[13] W. R. Rypniewski, S. Mangani, B. Bruni, P. L. Orioli, M. Casati, K. S. Wilson, *J. Mol. Biol.* **1995**, *251*, 282.
[14] I. Bertini, L. Banci, C. Luchinat, M. Piccioli, *Coord. Chem. Rev.* **1990**, *100*, 67.
[15] N. J. Blackburn, S. S. Hasnain, N. Binsted, G. P. Diakun, C. D. Garner, P. F. Knowles, *Biochem. J.* **1984**, *219*, 985.
[16] H. J. Prochaska, W. F. Schwindinger, M. Schwartz, M. J. Burk, E. Bernarducci, R. A. Lalancette, J. A. Potenza, H. J. Schugar, *J. Am. Chem. Soc.* **1981**, *103*, 3446.
[17] E. Bernarducci, P. K. Bharadwaj, R. A. Lancette, K. Krogh-Jespersen, J. A. Potenza, H. J. Schugar, *Inorg. Chem.* **1983**, *22*, 3911.
[18] E. Bernarducci, P. K. Bharadwaj, K. Krogh-Jespersen, J. A. Potenza, H. J. Schugar, *J. Am. Chem. Soc.* **1983**, *105*, 3860.
[19] S. Knapp, T. P. Keenan, X. Zhang, R. Fikar, J. A. Potenza, H. J. Schugar, *J. Am. Chem. Soc.* **1990**, *112*, 3452.
[20] J. A. Goodwin, D. M. Stanbury, L. J. Wilson, C. W. Eigenbrot, W. R. J. Scheidt, *J. Am. Chem. Soc.* **1987**, *109*, 2979.
[21] J. A. Goodwin, L. J. Wilson, D. M. Stanbury, R. A. Scott, *Inorg. Chem.* **1989**, *28*, 42.
[22] G. J. Kubas, *Inorg. Synth.* **1990**, *28*, 68.
[23] C. J. Pickett, *J. Chem. Soc. Chem. Commun.* **1985**, 323.
[24] F. E. Mabbs, D. Collison, *Electron Paramagnetic Resonance of d Transition Metal Compounds*, Elsevier, Amsterdam, **1992**, p. 218.
[25] R. R. Gagné, C. A. Koval, G. C. Lisensky, *Inorg. Chem.* **1980**, *19*, 2854.
[26] H. Bredereck, G Theilig, *Chem. Ber.* **1953**, *86*, 88.
[27] Crystallographic data (excluding structure factors) for the structures reported in this paper have been deposited with the Cambridge Crystallographic Data Centre as supplementary publication No. CCDC-1220-9. Copies of the data can be obtained free of charge on application to the Director, CCDC, 12 Union Road, Cambridge CB21EZ, UK (Fax: Int. code +(1223)336-033; e-mail: teched@chemcrys.cam.ac.uk).
[28] a) N. Walker, D. Stuart, *Acta Crystallogr.* **1983**, *A39*, 158; b) G. M. Sheldrick in *Crystallographic Computing 3* (Eds.: G. M. Sheldrick, C. Krueger, R. Goddard), Oxford University Press, **1985**, p. 175.
[29] A. J. Canty, E. E. George, C. V. Lee, *Aust. J. Chem.* **1983**, *36*, 415.
[30] J. F. Dobson, B. E. Green, P. C. Healy, C. H. L. Kennard, C. Pakawatchai, A. H. White, *Aust. J. Chem.* **1984**, *37*, 649.
[31] W. Clegg, S. R. Acott, C. D. Garner, *Acta Crystallogr.* **1984**, *C40*, 768.
[32] S. Flanagan, J. A. Gonzalez, J. E. Bradshaw, L. J. Wilson, D. M. Stanbury, K. J. Haller, W. R. Scheidt in *Bioinorganic Chemistry of Copper* (Eds.: K. Karlin, Z. Tyeklar), Chapman & Hall, New York, **1993**, p. 91.
[33] F. E. Mabbs, D. Collison, *Electron Paramagnetic Resonance of d Transition Metal Compounds*, Elsevier, Amsterdam, **1992**, p. 405.
[34] A. W. Addison in *Copper Coordination Chemistry: Biochemical and Inorganic Perspectives* (Eds.: K. D. Karlin, J. Zubieta), Adenine Press, New York, **1983**, p. 109.
[35] R. J. Dudley, B. J. Hathaway, P. G. Hodgson, *J. Chem. Soc. Dalton Trans.* **1972**, 882.
[36] E. M. Gouge, J. F. Geldard, *Inorg. Chem.* **1978**, *17*, 270.
[37] M. Munakata in *Copper Coordination Chemistry: Biochemical and Inorganic Perspectives* (Eds.: K. D. Karlin, J. Zubieta), Adenine Press, New York, **1983**, p. 473.
[38] C. Dennison, P. Kyritsis, W. McFarlane, A. G. Sykes, *J. Chem. Soc. Dalton Trans.* **1993**, 1959.
[39] A. C. McLaughlin, J. S. Leigh, *J. Mag. Res.* **1973**, *9*, 296.
[40] C. M. Groeneveld, J. van Rijn, J. Reedijk, G. W. Canters, *J. Am. Chem. Soc.* **1988**, *110*, 4893.
[41] R. A. Lieberman, R. H. Sands, J. A. Fee, *J. Biol. Chem.* **1982**, *257*, 336.
[42] M. W. Pantoliano, J. S. Valentine, L. A. Nafie, *J. Am. Chem. Soc.* **1982**, *104*, 6310.
[43] M. E. McAdam, E. M. Fielden, F. Lavelle, L. Calabrese, D. Cocco, G. Rotilio, *Biochem. J.* **1977**, *167*, 271.
[44] E. K. Hodgson, I. Fridovich, *Biochemistry* **1975**, *14*, 5299.
[45] E. M. Fielden, P. B. Roberts, R. C. Bray, D. J. Lowe, G. N. Mautner, G. Rotilio, L. Calabrese, *Biochem. J.* **1974**, *139*, 49.
[46] R. C. Bray, S. A. Cockle, E. M. Fielden, P. B. Roberts, G. Rotilio, L. Calabrese, *Biochem. J.* **1974**, *139*, 43.
[47] I. Bertini, C. Luchinat, R. Monnanni, *J. Am. Chem. Soc.* **1985**, *107*, 2178.
[48] J. A. Fee, C. Bull, *J. Biol. Chem.* **1986**, *261*, 13000.
[49] L. Banci, I. Bertini, B. Bruni, P. Carloni, C. Luchinat, S. Mangani, P. L. Orioli, M. Piccioli, W. Rypniewski, K. S. Wilson, *Biochem. Biophys. Res. Commun.* **1994**, *202*, 1088.
[50] P. Cofré, D. T. Sawyer, *Inorg. Chem.* **1986**, *25*, 2089.
[51] C. Strong St. Clair, H. B. Gray, J. S. Valentine, *Inorg. Chem.* **1992**, *31*, 925.
[52] H. A. Azab, L. Banci, M. Borsari, C. Luchinat, M. Sola, M. S. Viezzoli, *Inorg. Chem.* **1992**, *31*, 4649.
[53] J. A. Fee, P. E. DiCorleto, *Biochemistry* **1973**, *12*, 4893.
[54] G. D. Lawrence, D. T. Sawyer, *Biochemistry* **1979**, *18*, 3045.
[55] D. T. Sawyer, J. S. Valentine, *Acc. Chem. Res.* **1981**, *14*, 393.
[56] R. Osman, H. Basch, *J. Am. Chem. Soc.* **1984**, *106*, 5710.
[57] M. Rosi, A. Sgamellotti, F. Taranlelli, I. Bertini, C. Luchinat, *Inorg. Chem.* **1986**, *25*, 1005.
[58] P. Carloni, P. E. Blochl, M. Parrinello, *J. Phys. Chem.* **1995**, *99*, 1338.
[59] J. Peisach, W. G. Levine, W. E. Blumberg, *J. Biol. Chem.* **1967**, *242*, 2847.
[60] W. J. Ingledew, J. C. Cobley, *Biochim. Biophys. Acta* **1980**, *590*, 141.
[61] W. J. Ingledew, *Biochim. Biophys. Acta* **1982**, *683*, 89.
[62] A. G. Sykes, *Adv. Inorg. Chem.* **1991**, *36*, 377.
[63] F. N. Büchi, A. M. Bond, R. Codd, L. N. Huq, H. C. Freeman, *Inorg. Chem.* **1992**, *31*, 5007.
[64] F. A. Armstrong, J. N. Butt, K. Govindaraju, J. McGinnis, R. Powls, A. G. Sykes, *Inorg. Chem.* **1990**, *29*, 4858.
[65] A. G. Sykes, *Struct. Bond.* **1991**, *75*, 175.
[66] H. B. Gray, *Chem. Soc. Rev.* **1986**, *15*, 17.
[67] D. Richardson, *Inorg. Chem.* **1990**, *29*, 3213.
[68] M. Born, *Z. Phys.* **1920**, *1*, 45.
[69] R. J. Kassner, W. Yang, *J. Am. Chem. Soc.* **1977**, *99*, 4351.
[70] M. R. McDevitt, A. W. Addison, *Inorg. Chim. Acta.* **1993**, *204*, 141.
[71] J. A. Guckert, M. D. Lowery, E. I. Solomon, *J. Am. Chem. Soc.* **1995**, *117*, 2817.
[72] S. E. Shadle, J. E. Penner-Hahn, H. J. Schugar, B. Hedman, K. O. Hodgson, E. I. Solomon, *J. Am. Chem. Soc.* **1993**, *115*, 767.
[73] S. Dahlin, B. Reinhammar, M. T. Wilson, *Biochem. J.* **1984**, *218*, 609.
[74] C. M. Groeneveld, G. W. Canters, *J. Biol. Chem.* **1988**, *203*, 167.
[75] C. M. Groeneveld, M. C. Ouwerling, C. Erkelenes, G. W. Canters, *J. Mol. Biol.* **1988**, *200*, 189.
[76] A. Lommen, G. W. Canters, *J. Biol. Chem.* **1990**, *265*, 2768.
[77] D. G. A. Harshani de Silva, D. Beoku-Betts, P. Kyritsis, K. Govindaraju, R. Powls, N. P. Tomkinson, A. G. Sykes, *J. Chem. Soc. Dalton Trans.* **1992**, 2145.
[78] A. M. Q. Vande Linde, K. L. Juntunen, O. Mols, M. B. Ksebali, L. A. Ochrymowycz, D. B. Rorabacher, *Inorg. Chem.* **1991**, *30*, 5037.
[79] D. K. Coggin, J. A. González, A. M. Kook, C. Bergman, T. D. Brennan, W. R. Scheidt, D. M. Stanbury, L. J. Wilson, *Inorg. Chem.* **1991**, *30*, 1125.
[80] C. M. Groeneveld, G. W. Canters, *Eur. J. Biochem.* **1985**, *153*, 559.
[81] G. Van Pouderoyen, S. Mazumdar, N. I. Hunt, H. A. O. Hill, G. W. Canters, *Eur. J. Biochem.* **1994**, *222*, 583.
[82] A. Aitken, *Biochem. J.* **1975**, *149*, 675.